Journal of Applied Electrochemistry (2005) 35:599–607
DOI 10.1007/s10800-005-2320-5

On the electrochemical flow measurements using carbon-based screen-printed electrodiffusion probes

XAVIER ADOLPHE[1], SERGUEI MARTEMIANOV[1,*], ILARIA PALCHETTI[2] and MARCO MASCINI[2]
[1]*Laboratory of Heat Studies-LET, UMR CNRS 6608, ESIP, University of Poitiers, 40 Avenue du Recteur Pineau, 86022, Poitiers Cedex, France*
[2]*Dipartimento di Chimica, Università degli Studi di Firenze-Polo Scientifico, Via della Lastruccia 3, 50019, Firenze, Italy*
*(*author for correspondence, fax: +33-5-49-45-35-39; e-mail: serguei.martemianov@univ-poitiers.fr)*

Received 1 June 2004; accepted in revised form 1 February 2005

Key words: electrochemical flow measurements, screen-printed probes, mass flux, near-wall turbulence, wall shear stress, impedance

Abstract

In this article, we have studied the possibility of using carbon-based screen-printed probes for electrochemical flow and mass flux measurements. Such probes have, up to now, been mainly used as biosensors to study *in vivo* reactions. Our study shows that screen-printed sensors allow the measurement of mass flux and mean wall shear stress with good accuracy and high reproducibility. The existence of a micro-porous layer covering the surface of screen-printed electrodes has been revealed by means of the impedance measurements and has been confirmed by Scanning Electron Microscopy. This layer influences the statistical characteristics of the turbulent limiting diffusion current and should be taken into account as an additional transfer function between the current and the velocity fluctuations. The use of screen-printed sensors opens new possibilities in the field of electrochemical flow diagnostics. The advantage of this new manufacturing technology lies in the possibility of serial mass production at very competitive prices (disposable sensors) combined with the possibility of the manufacture of segmented electrodes or matrix of electrodes. These new possibilities can be used for various industrial applications as well as for scientific studies on near-wall turbulent mass transfer. Furthermore, it is possible to envisage the development of a hybrid sensor (electrodiffusional/biochemical) allowing the study of *in situ* biochemical reactions in a flow.

Nomenclature

A	microelectrode area, $A = \pi\, d^2/4$[m^2]	$\bar{H}$	$H(f)/H(f\rightarrow 0)$ normalizing form of the transfer function
C	concentration of electroactive species, [mol m^{-3}]	I	limiting diffusion current, [A]
C_w	concentration of electroactive species at the interface, [mol m^{-3}]	I'	fluctuations of limiting diffusion current, [A]
C_∞	bulk concentration of electroactive species, [mol m^{-3}]	I_o	residual current,[A]
D	diffusion coefficient, [m^2 s^{-1}]	J	mass flux to the wall, [mol s^{-1}]
d	diameter of circular microelectrode, [m]	j	imaginary unit, $\sqrt{-1}$
d_h	hydraulic diameter of channel, [m]	K	mass transfer coefficient, [m s^{-1}]
F	Faraday number, $F = 96500$, [C mol^{-1}]	L	distance in the pressure drop Δp measurements, [m]
f	frequency, [Hz]	n	number of electrons transferred in the electrochemical reaction
f_r	electrochemical roughness coefficient		
$H(f)$	the transfer function	SP_1, SP_2	screen-printed electrodes

t	time, [s]
U	flow velocity, [m s^{-1}]
$W_{ii'}$	power spectral density (PSD) of the limiting diffusion current fluctuations, [A^2 s]
$\overline{W}_{ii}$	$W_{ii'}/W_{ii'}(f\rightarrow 0)$ normalizing form of PSD of limiting diffusion current
$W_{\tau\tau'}$	power spectral density of the wall shear stress fluctuations, [Pa^2 s]
Z	Impedance, [Ohm^{-1}]

Dimensionless group

$Sc = \nu/D$	SCHMIDT number
$Re = Ud_h/\nu$	REYNOLDS number

Greek symbols

β	Cottrell coefficient, [A $s^{1/2}$]
δ_d	diffusion layer thickness, [m]
ε	rate of the current fluctuations
ζ	Leveque coefficient, [A $Pa^{-1/3}$]
λ	skin friction coefficient
μ	dynamic viscosity, [Pa s]
$\nu = \mu/\rho$	kinematic viscosity, [m^2 s^{-1}]
$\sigma = 2\pi f(d^2\mu^2/D^{-2}\tau)^{1/3}$	dimensionless frequency for a circular microelectrode
τ	longitudinal shear stress at the wall, [Pa]
ϕ	phase shift

Superscripts

–	average value
∞	bulk
w	electrode surface
exp	experimental
th	theoretical
| |	modulus

1. Introduction

The study of near-wall flow dynamics and transfer phenomena necessitates the development of reliable sensors. Electrochemical flow diagnostics are well adapted for mass flux and wall shear stress measurements [1]. Nevertheless, practical applications of this method are limited in some cases by the manufacture of suitable sensors. There are problems related to mass flux measurements on curved surfaces, with the manufacture of segmented electrodes for flow direction measurements and with the manufacture of sensor matrixes for near turbulence studies. The development of technologies for the mass production of reliable and inexpensive electrochemical sensors for flow diagnostics is an open question.

Over the last few years, the manufacture of electrochemical sensors has undergone a remarkable renewal. New innovating technologies have been proposed for the manufacture of electrochemical probes: photolithography [2], silicon technology [3, 4] and three-segmented probes technique [5]. In particular, photolithography enables the mass production of sensors, with the advantage of scrutinizing near interface phenomena at an ever-lower scale. However, the use of the photolithography technique requires complex and expensive equipment and specifically-trained personnel for their implementation. Recently, Mascini and coworkers [6, 7] have set up a new sensor manufacturing process that is less complex, low-cost, and which can answer practical needs, under the name 'Screen Printed Technology'. Today the screen-printed electrodes are mainly used as biosensors.

The advantages of screen printing are numerous: disposable sensors, mass production, the possibility of producing the sensors on a plastic substrate, different surface geometry of sensitive probes, etc. In the present study, we will stress the possibility of adapting screen-printed sensors for electrochemical flow measurements of local wall shear stress and their use as mass flux-meters for the study of near wall transfer phenomena.

Most industrial flows are turbulent. Particular attention was drawn to the study of wall turbulence in the viscous sublayer [8–10], because the mass transport in this zone determines numerous electrochemical and physicochemical engineering processes. Most traditional experimental methods such as Laser Doppler Anemometry (LDA), Particle Image Velocimetry (PIV), Thermo anemometry, cannot be used successfully in the near vicinity to the wall. But the electrochemical method seems well adapted to measurements in the viscous sublayer. As a matter of fact, Hanratty and Reiss [8], Shaw and Hanratty [11] have demonstrated that flush mounted with the solid surface electrode allows measurement of the instantaneous local values of the mass flux to the wall. Determining the instantaneous local wall velocity gradient is a much more complicated problem which requires, in general, resolution of the inverse problem. Nevertheless some simplified approaches exist which allow the determination of the power spectral density of the local wall shear stress fluctuations. These approaches are based on the use of the transfer function which is calculated theoretically for an 'ideal' electrode. In the present work particular attention was paid to the experimental study of the transfer function of the real screen-printed electrode. This allows us to spread the field of applications of screen-printed sensors to near wall turbulence studies. On the other hand, investigation of the frequency response of electrochemical probes on turbulent perturbations is a very promising way of studying fine surface structure and morphology.

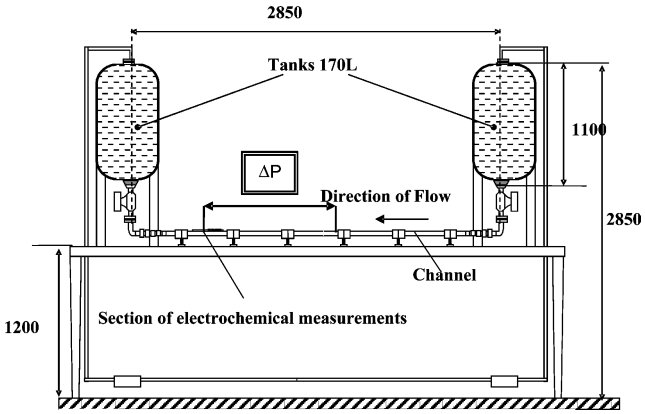

Fig. 1. Hydro-electrochemical channel.

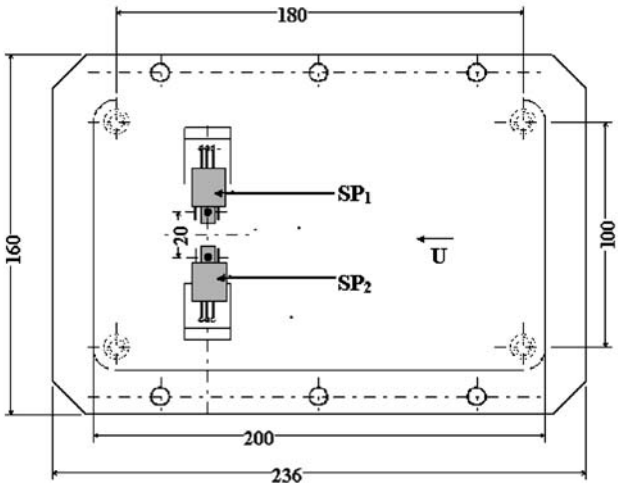

Fig. 3. Section of measurements with screen-printed sensors.

The understanding of near interface transfer phenomena requires knowing the active area of the electrode. Combination of the Cottrell method with the electrochemical impedance measurements is an efficient tool for determining and for the control of the active electrode area. In the present work, this experimental tool is used to account for the reliability and the reproducibility of our experimental measurements. The Cottrell measurements give directly an effective surface area which is the important parameter for mass flux and local wall shear stress measurements. The impedance measurements allow fine control of the electrode–solution interface state and can be used to identify changes of status of the electrode surface over time.

2. Description of the experiments

Experiments were conducted in a two-dimensional rectangular Plexiglas channel with a cross section of 120 mm × 12 mm, Figure 1. This channel was placed between two tanks (≅170 l). Flow through the channel was achieved by imposing overpressure. The flow rate was measured by means of on electromagnetic flow meter, and the pressure drop by means of a differential manometer. The measurement section with the electrochemical sensors was located 2 m downstream of the right tank to ensure well developed turbulent flow conditions in the range of the Reynolds numbers investigated (Re∈[10,000–40,000]).

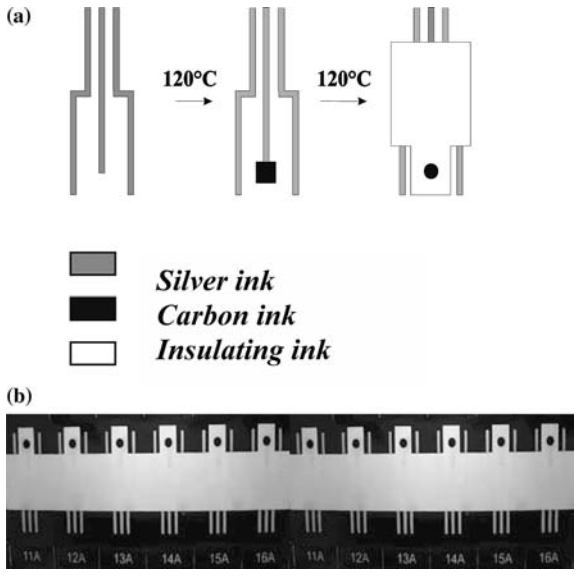

Fig. 2. Screen-printed sensors: stages of manufacturing (a) and band of sensors (b).

The liquid used was a 25 mol m^{-3} aqueous solution of $K_3Fe(CN)_6$ and $K_4Fe(CN)_6$, with a 300 mol m^{-3} of K_2SO_4 as the supporting electrolyte. The temperature during the experiments was maintained in 21.0 ± 0.1 °C, the value of the kinematic viscosity (ν) is 9.7×10^{-7} m^2 s^{-1}. Molecular diffusion coefficient (D) of electroactive species was obtained using the rotating disc electrode measurements, for the cathodic polarization its value was equal to $D = 7.07 \times 10^{-10}$ m^2 s^{-1}. So, the Schmidt number ($Sc = \nu/D$) was about 1400. The electrodiffusion measurements were realized by applying a voltage between two electrodes, a working electrode (SP_1 or SP_2) and a large counter electrode. The diameter of working electrodes was $d = 3$ mm.

Working electrodes were manufactured by using the 'Screen-Printed Technology' method. Using this technology a great number of various sensors and planar transducers characterized by a high mechanical resistance have been made: thermal sensors, chemical sensors, biosensors and others [3, 4, 6–7]. This technology consists of deposing inks on a substrate in a film of controlled pattern and thickness. It is thus possible to produce electrodes of very different shapes. Different inks can be used to print electrodes based on noble metals (Au, Pt, Ag, etc.) and therefore different properties of the final sensor can be obtained. However, for these inks a high firing temperature (850–1200 °C) is necessary and the overall process becomes cumbersome. For our sensors, the polymeric carbon-based inks were used, because of their very low firing temperature (from

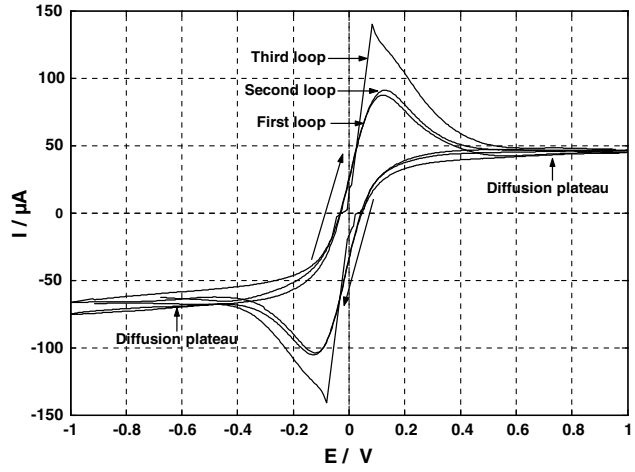

Fig. 4. Voltage-current curves for screen-printed electrode.

room temperature to 120 °C) and because they can be printed on several kind of supports like glass, ceramic and plastic sheets. A graphite based ink, a silver ink, a silver–silver chloride ink, and an insulating ink were used during the manufacture. At first the silver tracks were printed, then the graphite pad was positioned over part of the silver track and finally the insulating layer was deposited with openings that allow electrical contact with the external circuit, Figure 2a. After each printing step the inks were heated at 110 °C during 10 min for polymerization.

The final product of the screen-printed technology is a band of electrodes on the flexible substrate, see Figure 2b. These electrodes can be easily fixed on the wall in the place where the electrochemical flow measurements should be taken.

In our experiments two carbon-based screen-printed circular electrodes (SP_1 and SP_2) were sticks on the wall of the measuring section at a distance of 20 mm one-to-one, flush in the direction of flow, Figure 3. All electrodiffusional measurements were performed after 30 min of immersion of the electrodes in the solution. This time was necessary for stabilization of the sensor's characteristics (the reasons will be explained later).

3. Mass flux and wall shear stress measurements

In the diffusion regime, Faraday's law allows us to link the mass flux to the wall of electroactive ions (J) to the electrical current of the external circuit (I)

$$I = nFJ \tag{1}$$

where n is the number of electrons which take part in the electrochemical reaction and F is the constant of Faraday. The existence of the diffusion regime can be confirmed by measurements of voltage–current curves.

Measurements of the voltage–current curves for screen-printed sensors were taken in the hydraulic channel using a potentiostat (SOLARTRON SI 1480A MultiStat.) and software 'Corrwarre'. This software controls all functions of the potentiostat and allows the processing of the experimental curves. Figure 4 presents three consecutive voltage–current loops obtained with the scanning rate of 7 mV s^{-1}. The experiments were carried out in motionless solution. The voltage–current measurements in flow were impossible. Indeed the manipulation time for our installation is limited by the tank's volume.

Current–voltage curves have strong overshoots close to the equilibrium potential and two horizontal diffusion plateaus which correspond to the limiting diffusion currents in the regime of cathodic and anodic polarization. These plateaus are located in the intervals of potential between [1;−0.4] Volt/Pt and [0.5; + 1.] Volt/Pt. The existence of overshoot shows that the kinetic resistance of our electrodes is rather high, which is not surprising. But the existence of well defined diffusion plateaus supports the possibility of using screen-printed sensors for mass transfer and flow measurements.

The current–voltage curves change with time during the first moments. One of the possible explanations is the existence of a micro porous structure on the surface of the screen printed electrodes. This structure can be seen on the picture of a screen-printed electrode obtained by Scanning Electron Microscopy, Figure 5. After the immersion of the electrode into solution some time is necessary for filling the micro porous layer with

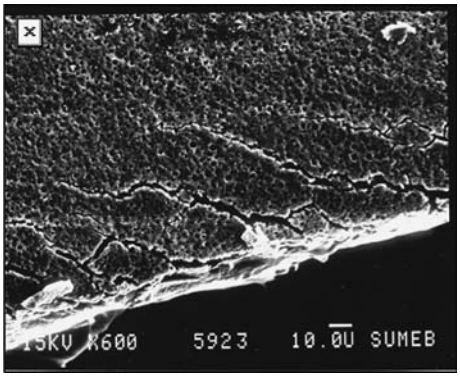

Fig. 5. Image of screen-printed electrode obtained by Scanning Electron Microscopy (SEM).

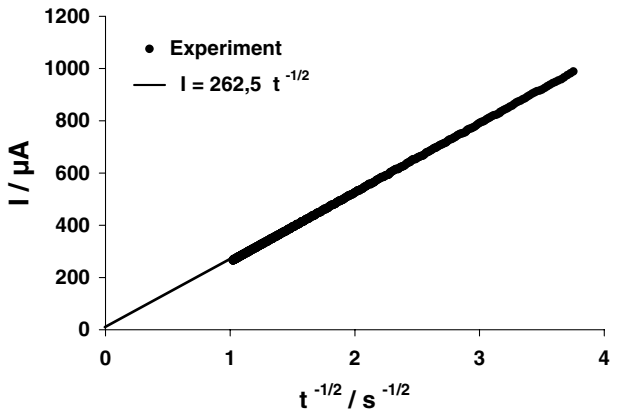

Fig. 6. Voltage-step transient curve for screen-printed electrode (Cottrell method).

Table 1. Standard deviation of the active surface area for seven screen-printed electrodes.

Screen-printed electrode	β/μA s $^{1/2}$	Active area A/mm^2 calculated from β	Roughness factor
1	262.5	7.25	1.02
2	254.5	7.03	0.99
3	254.0	7.02	0.99
4	242.0	6.69	0.95
5	262.5	7.25	1.02
6	259.5	7.17	1.01
7	244.0	6.74	0.95
Average value	254.1	7.02	0.99
Standard deviation	8.3 (≈ 4 %)	0.23 (≈ 4 %)	0.03 (≈ 4 %)

the electrolyte. This time was estimated by means of impedance measurements (see paragraph 5) and is about 30 min. So before starting mass flux and flow measurements, the electrodes were maintained immersed in the solution for half an hour beforehand to take the electrochemical system towards a stable state.

Under the limiting diffusion current conditions the concentration of the electroactive species on the surface of the working electrode is equal to zero ($C_w = 0$), so we know exactly the concentration gradient. This opens the way to determine the mass transfer coefficient $K = J/A\Delta C$, where A is the area of the working electrode.

The surface area of the electrode, on which the exchange of electrons is carried out, is essential to determine the value of the mass transfer coefficient. It is necessary to make the distinction between the geometrical surface obtained by an optical technique and the active surface (or real electrochemical surface). The ratio of electrochemical surface to the geometrical surface can be characterized by the coefficient f_r (called 'electrochemical roughness' in [12]).

The voltage-step transient method, more usually called the Cottrell method [13], makes it possible to obtain the active surface of an electrode. The method is based on the application of a voltage step (which corresponds to the diffusion plateau) with the following recording of the evolution of the current with time. Software ED-WORK98 [14] was used for the signal processing to provide transient curves.

For the short times the measured diffusion current $I(t)$ can be confronted [14, 15] with the relation:

$$I = \beta t^{-\frac{1}{2}}, \qquad (2)$$

obtained from the resolution of the non-stationary linear diffusion equation. In Equation (2) the coefficient $\beta = nFAC_\infty(D/\pi)^{0.5}$, where A is the active surface of the electrode and c_∞ is the bulk concentration. Thus, the slope β in the Equation (2) enables us to obtain the active surface of the electrode A, if the diffusion coefficient D is known.

Figure 6 shows, as an example, the results of the Cottrell measurements for the screen-printed electrode SP_1 which were taken in the hydraulic channel in

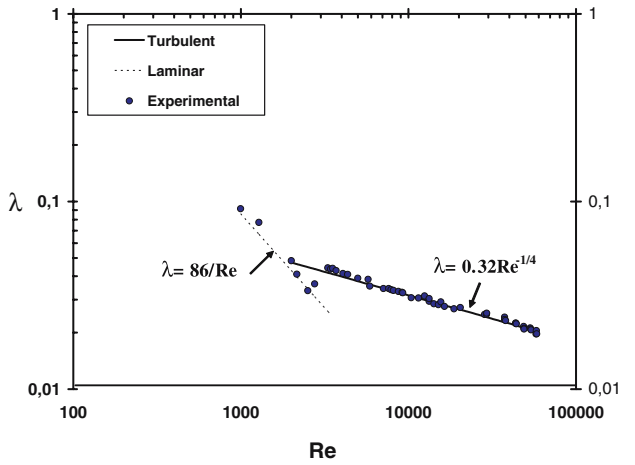

Fig. 7. Hydraulic calibration curve.

motionless solution. Using the Cottrell measurements, we obtained 7.25 mm^2 and 7.03 mm^2 as the active surface area and 1.03 and 0.99 as the 'roughness factor' f_r for the electrodes SP_1 and SP_2. In order to estimate the reproducibility of the active surface area of the screen-printed sensors we have submitted to the Cottrell test five other electrodes taken at random in the same manufacturing band, see Figure 2a. The results are presented in Table 1, where the two first lines correspond to the electrodes SP_1 and SP_2. It is possible to see that the standard deviation for the active surface area is about 4%. So, within the accuracy of our measurements (we estimate experimental errors for the Cottrell measurements as 5%) the screen-printed electrodes taken at random in the same manufacturing band have well reproducible active surface. The roughness factor for the tested electrodes was about 1, it means that the active surface can be identified with the geometrical surface. Nevertheless, we are not sure that this conclusion is general. The active surface area can be influenced by roughness (it leads to $f_r > 1$) and by the presence of

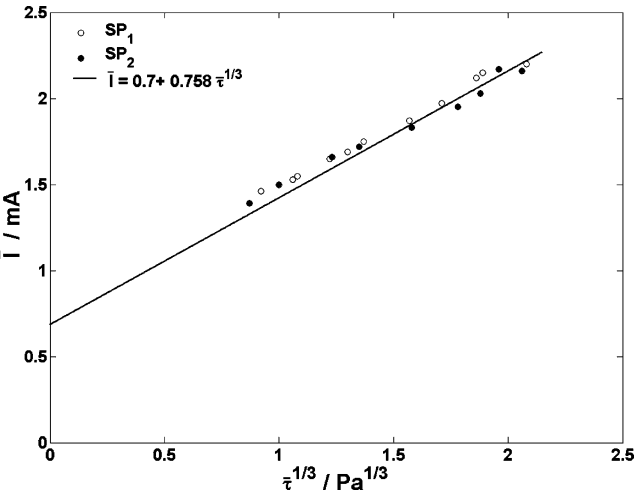

Fig. 8. Dependence of the limiting diffusion current on the wall shear stress.

inactive patches over the macroscopic area of the electrode (it can lead to $f_r < 1$). For various manufacturing bands these two factors can be of different importance. That is why the use of screen-printed electrodes for electrodiffusional measurements should be accompanied by the Cottrell test.

Thanks to the work of Leveque [16], we can relate for the circular electrode the mean limiting diffusion current ($\bar{I}$) to the mean local wall shear stress ($\bar{\tau}$):

$$\bar{I} = \zeta_{th}\bar{\tau}^{+\frac{1}{3}}, \tag{3}$$

where $\zeta_{th} = 0.68\mathrm{F}D^{2/3}C_\infty\mu^{-1/3}d^{5/3}$ and d is the probe diameter. For our experimental conditions and for the probe diameter $d = 3$ mm, the constant is equal to $\zeta_{th} = 0.80$ mA Pa$^{-1/3}$.

Our installation allows us to determine the local shear stress in the section of electrochemical measurements by measuring the pressure drop ΔP between two points located on the distance $L = 1.15$ m:

$$\bar{\tau} = \frac{\Delta P d_h}{4L}. \tag{4}$$

Indeed, the section of electrochemical measurement is located at 90 hydraulic diameters from the channel entry, so hydrodynamical characteristics can be considered as uniform along the flow. We present in Figure 7 the results of hydraulic measurements, namely the skin friction coefficient $\lambda = 8\bar{\tau}/\rho U^2$, obtained by the pressure drop measurements. This chart can be interpreted as the hydraulic calibration curve for our channel. It is noted that obtained hydraulic law λ(Re) corresponds to well known relations for turbulent and laminar flows in a rectangular channel with the aspect ratio 0,1 [17]:

$\lambda = 0.32\mathrm{Re}^{\frac{-1}{4}}$ for the turbulent regime;

$\lambda = 86\mathrm{Re}^{-1}$ for the laminar regime.

Thus, we have the possibility to plot the dependence of the limiting diffusion current on the wall shear stress, see Figure 8. This figure shows that the limiting diffusion current for screen-printed electrodes can be fitted by the equation:

$$\bar{I} = \bar{I}_0 + \zeta_{exp}\bar{\tau}^{\frac{1}{3}}, \tag{5}$$

where the slope ζ_{exp} is equal to $\zeta_{exp} = 0.758$ mAPa$^{-1/3}$. The experimental value ζ_{exp} is approximately the same for both electrodes (SP_1 and SP_2) and is slightly different from the theoretical constant ζ_{th} (within 10% accuracy). The term I_0 in Equation (5) corresponds to the kinetic resistance of screen-printed electrodes, which is probably due to the influence of the micro porous layer.

Use of screen-printed probes for the wall shear stress measurements should involve a procedure of calibration of these sensors. In this sense, Figure 8 can be considered as the calibration curve. This curve is analogue to the King'law in the thermoanemometrical method.

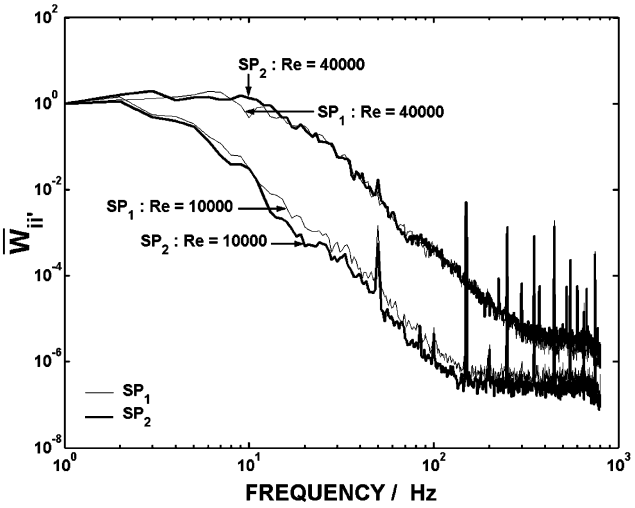

Fig. 9. PSD of the limiting diffusion current $\bar{W}_{ii}$ of two screen-printed electrodes at two Reynolds numbers.

4. Spectral analysis of mass flux and wall shear stress fluctuations

In turbulent flows the limiting diffusion current breaks up into an average and a fluctuating value, $I = \bar{I} + I'$. Through Faraday's law, Equation (1), the current fluctuations are directly proportional to the mass flux fluctuations. The mass flux on the wall is proportional to the concentration gradient, so statistical analysis of current fluctuations allows us to obtain important information concerning the turbulent transfer characteristics within the viscous sublayer [1, 10, 11, 18–23]. The detailed study of the near wall turbulent transfer is possible by using a matrix of measuring electrodes [19]. Manufacture of such an experimental device by means of traditional techniques poses a number of problems. On the other hand, screen-printed technology is well adapted for the manufacture of the electrode arrays of different geometries. This fact justifies our interest in measurements of turbulent fluctuations of limiting diffusion current of screen-printed electrodes.

The intensity of the current fluctuations

$$\varepsilon = \frac{\sqrt{\overline{I'^2}}}{\bar{I}}, \tag{6}$$

obtained with screen-printed electrodes is around 13% for Re = 10,000 and around 9 % for Re = 40,000. This intensity corresponds to the one obtained with a Pt electrode in the same experimental conditions.

Figure 9 presents the power spectral density (PSD) of the limiting diffusion current fluctuations W_{ii} (f) obtained by means of two screen printed electrodes at Reynolds number 10,000 and 40,000. Thereafter we use the normalising form of the PSD:

$$\overline{W}_{ii} = \frac{W_{ii}(f)}{W_{ii'}(f \to 0)}, \tag{7}$$

In accordance with the traditional notions an increase in the Reynolds number translates into the development of

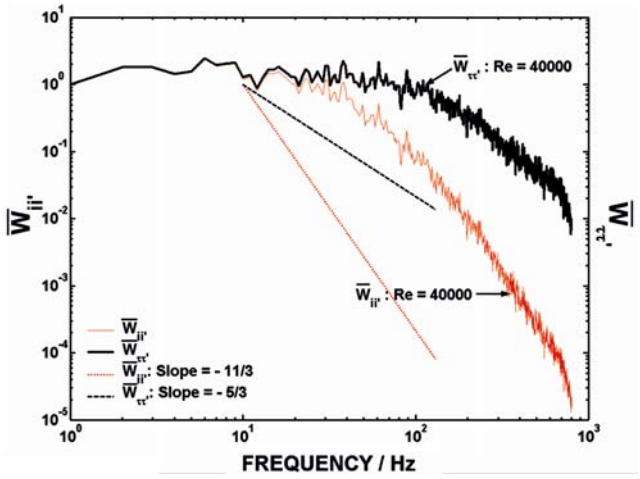

Fig. 10. PSD of current $\bar{W}_{ii}$ and wall shear stress $\bar{W}_{\tau\tau}$ fluctuations obtained by means of a circular platinum electrode at Re = 40,000.

the energy cascade. Moreover, the frequency evolution of the PSD is practically identical for both electrodes. This fact confirms the reliability of the screen-printed electrodes with respect to turbulent studies.

Usually the PSD of the limiting diffusion current fluctuations W_{ii} is linked with the PSD of the wall shear stress fluctuations $W_{\tau\tau}$ through the following relation:

$$W_{ii}(f) = |H(f)|^2 W_{\tau\tau}(f), \tag{8}$$

where $H(f)$ is the transfer function of the diffusion layer.

For the smooth ('ideal') electrode the transfer function $H(f)$ was calculated analytically and numerically [1, 18, 20]. Thereafter, for the normalising form of the transfer function $\bar{H}(\sigma)$ we will use Equations (10, 11) proposed in [20] for the circular probes:

$$\bar{H}(\sigma) = \frac{|H(\sigma)|}{|H(0)|} = (1 + 0.049\sigma^2 + 0.0006\sigma^4)^{-0.5} \quad \text{for } \sigma \le 6; \tag{9}$$

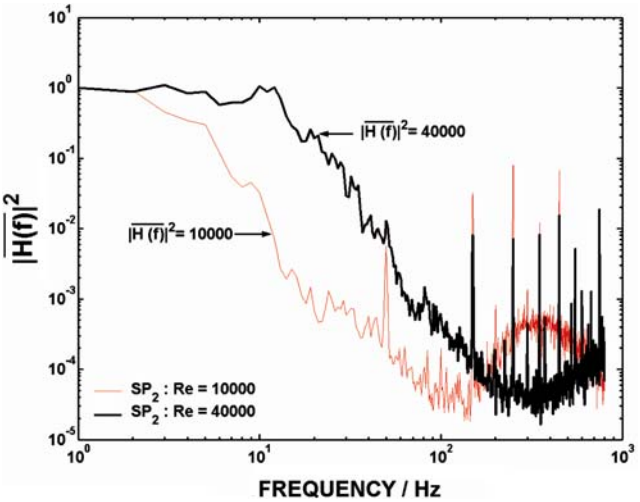

Fig. 11. Transfer function of screen-printed electrode SP_2 at two Reynolds numbers.

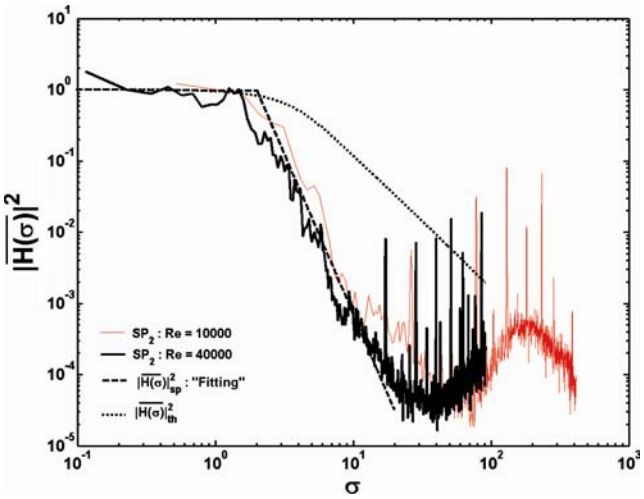

Fig. 12. Comparison of transfer functions for screen-printed electrode $|\overline{H(\sigma)}|^2_{SP}$ and for "ideal" electrode $|\overline{H(\sigma)}|^2_{TH}$.

$$\bar{H}(\sigma) = \frac{|H(\sigma)|}{|H(0)|} = \frac{\sqrt{(5.3\sqrt{2})^2 + (5.3\sqrt{2} - 8.832\sqrt{\sigma})^2}}{2\sigma^{\frac{3}{2}}} \quad \text{for } \sigma > 6; \tag{10}$$

with $\sigma = 2\pi f \left(\frac{d^2\mu^2}{D\bar{\tau}^2}\right)^{\frac{1}{3}}$ being the adimensional frequency, where d is the diameter of the probe.

Using the measurements of the PSD with smooth Pt electrode (d = 0.53 mm), see Figure 10, and the transfer function, Equations (9, 10), it is possible to calculate the PSD of the wall shear stress fluctuations in our channel. On Figure 10 we present, as an example, the results of the calculation of the normalising PSD of the wall shear stress fluctuations at Re = 40,000. We note that the PSD of the wall shear stress fluctuations decreases at high frequency range as $f^{-5/3}$. The same result has been obtained by [23] in the similar hydrodynamical conditions.

Using the calculating PSD of the wall shear stress fluctuations, the results of measurements with screen printed electrodes, Figure 9, and Equation (8) we can obtain the transfer function for screen printed electrodes $H_{SP}(f)$ at different Reynolds numbers. These results for the normalising form of the transfer function are presented on Figure 11. It is remarkable that using the adimensional frequency σ allows us to obtain a unique form for the transfer function, see Figure 12. For comparison we present on Figure 12 the transfer function of the 'ideal' electrode according to Equations (9, 10).

The transfer function of the screen printed electrodes can be fitted by the following analytical expressions:

$$|\overline{H(\sigma)}|^2 = \begin{cases} 1 \text{ for } \sigma \le 2 \\ (2/\sigma)^{9/2} \text{ for } \sigma > 2 \end{cases} \tag{11}$$

Finally, we can conclude that screen-printed electrodes can be used for studies of the near wall turbulent

transfer. However, the frequency response of these probes on hydrodynamic perturbations can be different from the ones obtained by the smooth Pt electrodes. From a practical point of view it means that transfer function will have to be rectified (see Equation (11)). Another possibility is related to the measurements which do not involve directly the use of the transfer function of electrochemical probes, as for example the space correlation or the delay time measurements [10].

Moreover, particularities in the frequency response of the screen-printed electrodes confirm that turbulent fluctuations can be used as an instrument for studies of the kinetics of the electrode's processes [24, 25]. Indeed, the difference between the frequency response of the screen-printed and platinum probes in the same hydrodynamic conditions can be interpreted as the additional hydro-electrochemical impedance [24] related to the morphology of screen-printed electrodes. Additional information about the fine structure of the screen-printed electrodes can be obtained by means of electrochemical impedance spectroscopy.

5. Electrochemical impedance of screen-printed electrodes

The principle of electrochemical impedance measurements rests on the analysis of electrode response to electrical sinusoidal perturbation at low amplitude. Electric signals of small amplitude make it possible to realize measurements in almost linear conditions and without modification of the system. In this work, the impedance measurements are used for two goals. The first one deals with the reliability of screen-printed probes. We use the impedance measurements for identification of possible changes in the electrode surface state in the course of time, which will account for the reliability of electrochemical flow measurements. The second goal is related to the comparative study of screen-printed and platinum electrodes in the same experimental conditions.

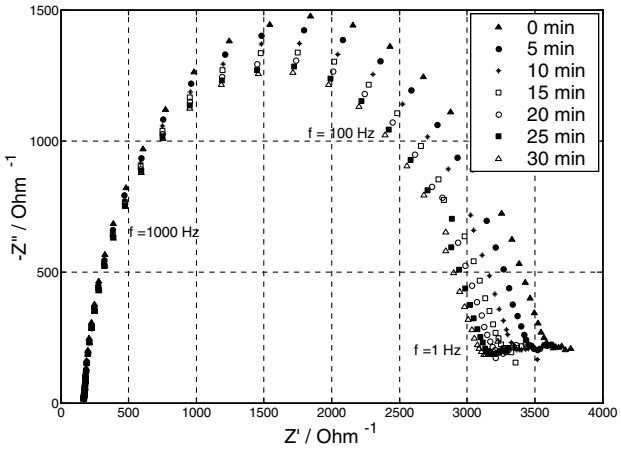

Fig. 13. Evolution of the impedance of the screen-printed electrode with time of immersion.

In the present study all impedance characteristics have been measured in the above mentioned ferri-ferrocyanide solution at the abandon potential by means of SOLARTRON SI 1480A MultiStat and a Frequency Response Analysers (FRA 1260). In order to specify the designations on the following figures, let us present the perturbation signal (potential) under the complex form:

$$X(t) = |X| \exp(j2\pi ft), \tag{12}$$

where $|X|$ and f are the signal amplitude and the frequency, j is the imaginary unit. The current response of the system to this perturbation will have the same form but with the phase shift for an angle:

$$Y(t) = |Y| \exp[j(2\pi f + \phi)]. \tag{13}$$

The electrochemical impedance which characterizes the system response in the frequency domain is defined by:

$$Z(f) = \frac{Y(f)}{X(f)} = |Z(f)| \exp(j\phi), \tag{14}$$

where $|Z(f)|$ is modulus of the impedance. It is also possible to present the impedance in the form of its imaginary and real part:

$$Z(f) = Z' + jZ'', \tag{15}$$

with $Z' = |Z(f)| \cos\phi$ and $Z'' = |Z(f)| \sin\phi$.

On Figure 13 the impedance of screen-printed probe SP_1 is presented for various times after the immersion of the electrode. We notice that Nyquist's diagram evolves in a significant way with the time of immersion. The electrode impedance does not change in the high frequency domain but decreases progressively and tends towards a limiting value in the low frequency domain. For law frequencies ($f < 10$ Hz) the electrode impedance is almost resistive. The impedance is stabilized at the end of 30 min of immersion. So we can speak about the evolution of the electrode/electrolyte interface with the following stabilization after 30 min of immersion.

For comparison we have measured the impedance of a platinum electrode ($d = 0.53$ mm) in the same operating conditions. The measurements did not indicate any evolution of the impedance in the course of time. Our experiments show also that the impedance of the screen-printed electrode is definitely superior to the platinum electrode.

We can explain the evolution of the screen-printed electrode impedance in time by a change in the surface state. This evolution concerns only the low frequencies that represent the interface impedance. Impedance in the high frequency domain which characterizes the resistance of the solution, remains unchanged whatever the electrode used.

It is confusing to compare directly the impedance characteristics of the screen-printed probe (diameter $d = 3$ mm) and a small Pt electrode ($d = 0.53$ mm) without scale compensation. Nevertheless, a qualitative comparison can be useful. It is known that for identical

conditions the impedance of electrochemical cell decreases with the working electrode size. Our experiments show inverse tendency, it means that interface of the screen-printed electrode possesses a supplementary resistance. This resistance that decreases with time can be attributed to the resistance of the porous layer covering the surface of the screen-printed sensor (see Figure 5). The time when the evolution of the impedance is observed can be interpreted as the necessary time for the filling of the micro-pores layer.

6. Conclusion

Our study demonstrated that carbon-based sensors fabricated by means of screen-printing technology can be successfully used for electrochemical flow diagnostics. In particular, these sensors allow the measurements of the mass flux and the mean wall shear stress on the surface. The effective surface area of these probes can be obtained from the voltage transient measurements and remains stable after 30 min immersion of the electrodes into electrolyte solution. The transient period of about 30 min is necessary for the stabilization of the sensor's characteristics due to the influence of the micro-porous layer covering the surface of the screen-printed electrodes. The existence of this layer has been revealed by means of the impedance measurements and has been confirmed by Scanning Electron Microscopy. Nevertheless, the existence of the micro-porous layer does not limit the use of the screen-printed sensors in the field of electrochemical measurements of the mass flux and the mean wall shear stress characteristics. The use of the screen printed electrodes for the local wall shear stress measurements should be accompanied by calibration in the known hydrodynamic conditions. Another possibility deals with the relative measurements.

The use of screen-printed sensors for studies of near wall turbulence and near wall turbulent mass transfer requires additional attention. These sensors can be directly applied for measurements of the characteristics which are not sensitive to the surface morphology of the probes (cross-correlations, delay-time, etc.). On the other hand, the micro-structure of the screen-printed sensors manifests itself as an additional transfer function between the fluctuating current and the fluctuating velocity. The detailed study of this transfer function is useful for two purposes:

- compensation of undesirable effects in PSD measurements of the wall shear stress fluctuations;
- development of hydro-electrochemical impedance method.

The practical advantages of screen-printed sensors are numerous. These sensors can be used for taking measurements in places of difficult access (curvilinear surfaces, thin layers), for multi-point measurements, etc. The advantage of this new manufacturing technology lies in the possibility of serial mass production at very competitive prices (disposable sensors) combined with the possibility of manufacturing segmented electrodes or matrix of electrodes with very varied forms. These new possibilities can be used for different industrial applications as well as for scientific studies on the near wall turbulence.

Acknowledgements

This work was supported by COST F2 programme "Electrochemical Sensors for Flow Measurements" of the European Science Foundation.

References

1. T.J. Hanratty, *Phys. Fluids* suppl, (1967) 126..
2. C. Deslouis, F. Huet, S. Robin and B. Tribollet, *Int. J. Heat Mass Transf.* **36** (1993) 829.
3. P. Bergveld, *Sensors Actuat. A: Phys.* **56** (1996) 65.
4. R.S. Sethi, *Biosens. Bioelectron.* **9** (1994) 243.
5. V. Sobolik, O. Wein, O. Gil and B. Tribollet, *Exp. Fluids* **9** (1989) 3198.
6. C. Capannesi, I. Palchetti, M. Mascini and A. Parenti, *Food Chem.* **71** (2000) 553.
7. I. Palchetti, M. Mascini, M. Minunni, A.R. Bilia and F.F. Vincieri, *J. Pharmaceut. Biomed. Anal.* **32** (2003) 251.
8. T.J. Hanratty and L.P. Reiss, *A.I.Ch.E. Journal* **8** (1962) 245.
9. B. Py, *Int. J. Heat Mass Transfer* **15** (1973) 129.
10. B.M. Grafov, S.A. Martemyanov and L.N. Nekrasov, *Turbulent Diffusion Layer in Electrochemical Systems* (Nauka publ, Moscow, 1990).
11. P.V. Shaw and T.J. Hanratty, *A.I.Ch.E. Journal* **10** (1964) 475.
12. J. Lore, A. Jardy, A. Falguieres and R. Rosset, *C.R. Acad. Sci. Paris* **274** (1972) 1979.
13. F.G. Cottrell, *Z. Physik. Chem.* **42** (1902) 385.
14. V. Sobolik, J. Tihon, O. Wein and K. Witcherle, *J. Appl. Electrochem.* **28** (1998) 329.
15. D.J. Macero and C.L. Ruffs, *J. Am. Chem. Soc.* **81** (1960) 2942.
16. J. Leveque, *Ann. Mines* **13** (1928) 201.
17. E. Idel'cik, "Mémento des pertes de charge", Paris, 'Eyrolles' Edition (1986).
18. E.F. Skurygin, S.A. Martemianov, M.A. Vorontyntsev and B.M. Grafov, *Sov. Electrochem.* **25** (1989) 685.
19. M.A. Vorotyntsev, S.A. Martemianov and B.M. Grafov, *J. Electroanal. Chem.* **179** (1984) 1.
20. C. Deslouis, O. Gil and B. Tribollet, *J. Fluid. Mech.* **215** (1990) 85.
21. A. Ambary, B. Tribollet and C. Deslouis, *Int. J. Heat Mass Transfer* **29** (1986) 35.
22. C. Deslouis, O. Gill and B. Tribollet, *Int. J. Heat Mass Transfer* **33** (1990) 2525.
23. J. Legrand, H. Aouabed, P. Legentilhomme and G. Lefebvre, *Exp. Therm. Fluid Sci.* **15** (1997) 125.
24. S.A. Martemianov and B.M. Grafov, *Sov. Electrochem.* **24** (1988) 344.
25. S.A. Martemianov and B.M. Grafov, *Sov. Electrochem.* **24** (1988) 1052.